Supporting Information for

Chemoaffinity-Mediated Synthesis of $NaRES_2$ Based Nanocrystals as Versatile Nano-Building Blocks and Durable Nano-Pigments

Yi Ding,[‡] Jun Gu,[‡] Tao Zhang, An-Xiang Yin, Lu Yang, Ya-Wen Zhang*, and Chun-Hua Yan*

Beijing National Laboratory for Molecular Sciences, State Key Laboratory of Rare Earth Materials Chemistry and Applications, PKU-HKU Joint Laboratory in Rare Earth Materials and Bioinorganic Chemistry, College of Chemistry and Molecular Engineering, Peking University, Beijing 100871, China.

Supplementary Experimental Section

Synthesis of $NaCeS_2$ nanocubes.

Method 1: elementary sulfur was used as the sulfurizing agent: Method 1 was described in the Experimental Section of the main text.

Method 2: H_2S gas was used as the sulfurizing agent: $Ce(Ac)_3 \cdot xH_2O$ (0.5 mmol), Na(acac) (4 mmol), OA (5 mmol), OM (17 mmol) and ODE (20 mmol) were loaded in a three-neck flask (100 mL). The mixture was heated to 110 °C under vacuum for 20 min to form Ce-oleate and Na-oleate, and then the flask was filled with absolute N_2. The mixture was heated to 250 °C, and H_2S – N_2 mixed gas was blown into the flask through a needle. The gas flow was fixed at 60 mL min^{-1}. The mixture was heated successively to 315 °C at a rate of 20 °C min^{-1} and kept at 315 °C for 5 min. The mixture generally turned from transparent light yellow solution to turbid red dispersion after kept at 315 °C for 1 to 3 min. After 5 min of heating, the NCs was air-cooled to room temperature and precipitated from the crude solution by ethanol (50 mL), followed by centrifugation and dispersion in cyclohexane.

Method 3: hot injection method: Na(acac) (6 mmol), OA (4 mmol), OM (17 mmol) and ODE (15 mmol) were loaded in one three-neck flask (100 mL), and $Ce(Ac)_3 \cdot xH_2O$ (0.5 mmol), OA (2 mmol) and ODE (5 mmol) were loaded in another three-neck flask (100 mL). The mixture in both flasks was heated to 110 °C under vacuum for 20 min to form Ce-oleate and Na-oleate, and then the flasks were filled with absolute N_2. The Na-solution was heated beyond 320 °C, and H_2S – N_2 mixed gas was blown into this flask through a needle. The gas flow was fixed at 60 mL min^{-1}. For typical synthesis, when the temperature of Na-oleate solution reached 322 °C or 326 °C, Ce-oleate solution was injected into the former one through a glass syringe quickly. The color of the mixture turned red as soon as the Ce-oleate solution was injected and the temperature dropped immediately. The mixture was kept at 315 °C for 5 min, and the NCs was air-cooled to room temperature and precipitated from the crude solution by ethanol (50 mL), followed by centrifugation and dispersion in cyclohexane.

Synthesis of $NaCe_xLa_{1-x}S_2$ nanocubes and $KCeS_2$ micro-crystals: $NaCe_xLa_{1-x}S_2$ nanocubes were synthesized in a similar way with Method 1, except that $Ce(Ac)_3 \cdot xH_2O$ (0.5 mmol) was replaced by $Ce(Ac)_3 \cdot xH_2O$ (0.25 mmol) and $La(acac)_3$ (0.25 mmol). Potassium

acetylacetonate (K(acac)) was prepared in a similar way with Na(acac) except that KOH was used instead of NaOH. $KCeS_2$ micro crystals were synthesized in a similar way with Method 1, except that Na(acac) (4 mmol) was replaced by K(acac) (4 mmol) and reaction time was extended from 10 min to 30 min.

Synthesis of $NaRES_2$ (RE = Dy to Lu, Y) nanocrystals: $RE(acac)_3$ (0.5 mmol), Sodium oleate (1 mmol), HDA (10 mmol) and ODE (10 mmol) were loaded in a three-neck flask (100 mL). The mixture was heated to 110 °C under vacuum for 20 min followed by filling the flask with pure N_2. H_2S – N_2 mixed gas was blown into this flask through a needle and the gas flow was fixed at 60 mL min^{-1}. The mixture was then heated to 280 °C and kept for 1 hour. The mixture generally turned form a light-yellow transparent solution to a white opaque dispersion after kept at 280 °C for 20 to 30 min. After 1 hour of heating, the NCs were air-cooled to room temperature and precipitated from the crude solution by ethanol (50 mL), followed by centrifugation and dispersion in cyclohexane.

Preparation of gold nanocrystals: Au NCs were synthesized through a modification method proposed by Klabunde and co-workers (Prasad, B. L. V.; Stoeva, S. I.; Sorensen, C. M.; Klabunde, K. J. *Langmuir* **2002**, *18*, 7515). 0.095 mmol of $HAuCl_4 \cdot H_2O$ and 0.235 mmol of dodecyldimethylammonium bromide (DDAB) were dissolved in 10 mL of toluene and sonicated for 5 min to form a homogeneous orange solution. Aqueous solution of $NaBH_4$ was prepared by dissolving 0.356 g $NaBH_4$ into of 1 mL of deionized water. Under vigorous stirring, 40 microliters of $NaBH_4$ solution was added dropwise into the toluene solution containing Au precursors. The solution turned purple within 2 min and was kept under vigorous stirring for 20 min. Then 0.8 mL of 1-docecanethiol was added into the solution and the reaction was kept for another 5 more minutes. The as-formed Au NCs were then collected from the crude solution by addition of 10 mL ethanol and centrifugation.

Preparation of NCs/PDMS materials: A 10:1:1 (volume ratio) mixture of SYLGARD silicone elastomer 184, the curing agent (Dow Corning Corp.), and a cyclohexane dispersion containing $NaCeS_2$ NCs were thoroughly mixed in a glass container and cured at 90 °C for 1 h in a vacuum oven. The composite materials with different types can easily be obtained through the mold or the cutting.

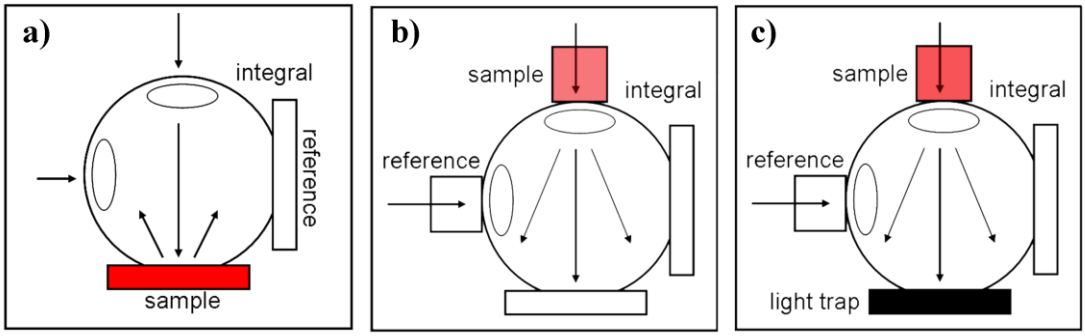

Figure S1. Schematic of a) diffuse reflection spectrum, b) total transmission spectra and c) scattering transmission spectra measurements.

Supplementary Data

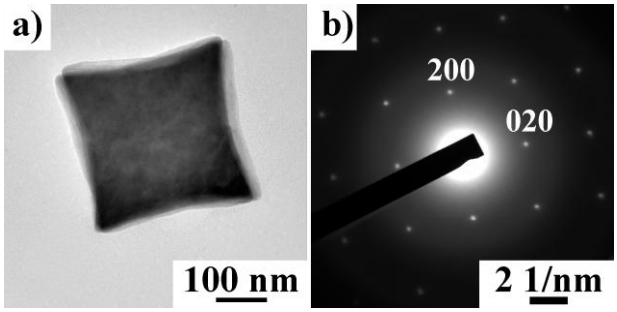

Figure S2. a) TEM image and b) corresponding selected area electron diffraction (SAED) pattern of a single $NaCeS_2$ nanocube.

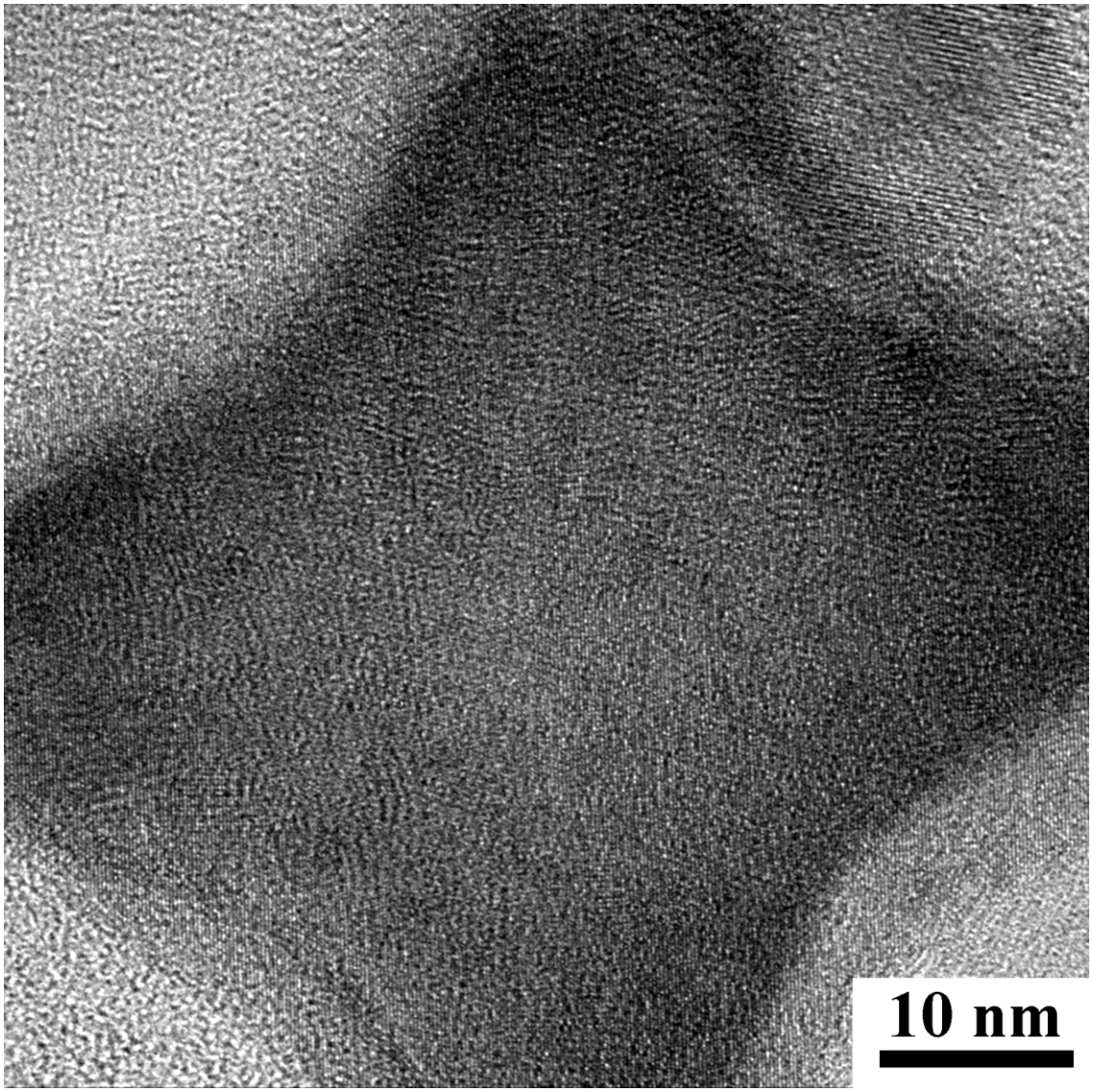

Figure S3. HRTEM image of a single $NaLaS_2$ NC with concave shape.

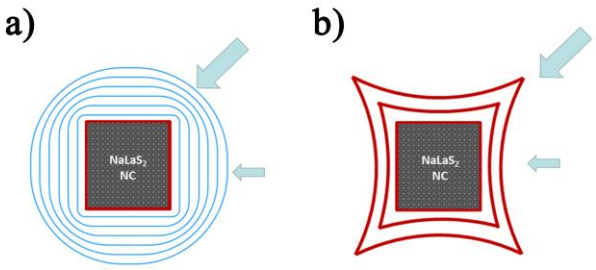

Figure S4. The diffusion controlled shape evolution of $NaLaS_2$ NCs. The two dimensional schematic illustration are used for simplicity; (a) blue lines indicate the different iso-surface of monomers' concentrations, *i.e.* each line represents locus with the same concentration; (b) red lines indicate the contour of the NCs during shape evolution. The blue arrow in both (a) and (b) indicates that the corners of the NCs receive more monomers than the facets due to the difference in concentration gradient.

Shape Evolution of $NaLaS_2$ NCs. Although the as-synthesized cubic phase $NaRES_2$ NCs generally have cubic morphologies, it is noteworthy that the bigger NCs (Figure 1d and 2a) possess the shape of concave nanocubes with pointy vertices, whereas the smaller NCs are normal nanocubes (Figure 1g-i and 2b). A further examination through HRTEM indicates that, unlike typical noble metal with concave shapes (Yu, T.; Kim, D. Y.; Zhang, H.; Xia, Y. *Angew. Chem. Int. Ed.* **2011**, *50*, 2773), the as-formed $NaRES_2$ NCs does not have specific facets (such as {310}, {510} facets) enclosing the crystal surfaces (Figure S3), which suggests that the shape of the NCs is more likely controlled by the diffusion-controlled shape evolution (Peng, Z. A.; Peng, X. G. *J. Am. Chem. Soc.* **2001**, *123*, 1389; Nielsen, A. E. *Kinetics of Precipitation*; Oxford: New York, 1964) instead of the specific binding of the capping agents. According to NC growth models (Talapin, D. V.; Rogach, A. L.; Haase, M.; Weller, H. *J. Phys. Chem. B* **2001**, *105*, 12278; Rempel, J. Y.; Bawendi, M. G.; Jensen, K. F. *J. Am. Chem. Soc.* **2009**, *131*, 4479), when the average distance between NCs are sufficiently large, each NC can be regarded as surrounded by a layer of undisturbed solution. In this layer of solution, the major force of transport is diffusion. According to classical crystal growth model,[S3] the linear growth velocity in diffusion control regime can be written as:

$$dr/dt = (Dv)cr^{-1} \quad \text{(S1)}$$

where r is the radius of the NCs, D is diffusion coefficient, v is the molecular volume, c is the concentration of the monomer. In a typical diffusion-controlled regime, each individual nanocube has a non-spherical distributed concentration gradient of the monomers (Figure S4a, the blue lines indicates the iso-surface of monomer's concentrations), which is higher close to the vertices than at the middle of the flat surface, *i.e.* {200} facets. As a result, the flux in the transport of monomers to the vertices is higher. The vertices thus have a higher linear growth rate, leading to the concave shape of the NCs (Figure S4b, red lines indicate the gradual changes of the contour of NC). If we reduce the monomer concentration, the size of the nanocubes should be reduced; and more distinguishably, the diffusion controlled process should be suppressed, and the shape of NCs should also change from concave to normal. While a typical synthetic conditions described in Experimental Section were based on the same ratio between the metal precursors, *i.e.* Na(acac) : $La(acac)_3$ = 8 : 1 (4 mmol : 0.5 mmol), when we further reduced the amount of $La(acac)_3$ in the precursors (*e.g.* Na(acac) : $La(acac)_3$ = 4 mmol : 0.3 mmol) to reduce diffusion controlled growth, the as-obtained $NaLaS_2$ NCs were smaller and no longer possessed concave morphologies;

instead, they were mainly regular cubic shape or cubic shape with rounded vertices (Figure 2b). This phenomenon can thus prove that the shape evolution between concave and regular nanocubes was indeed diffusion-controlled and the control over the growth regimes (*i.e.* diffusion and reaction) could not only influence the sizes but also the shapes of the NCs.

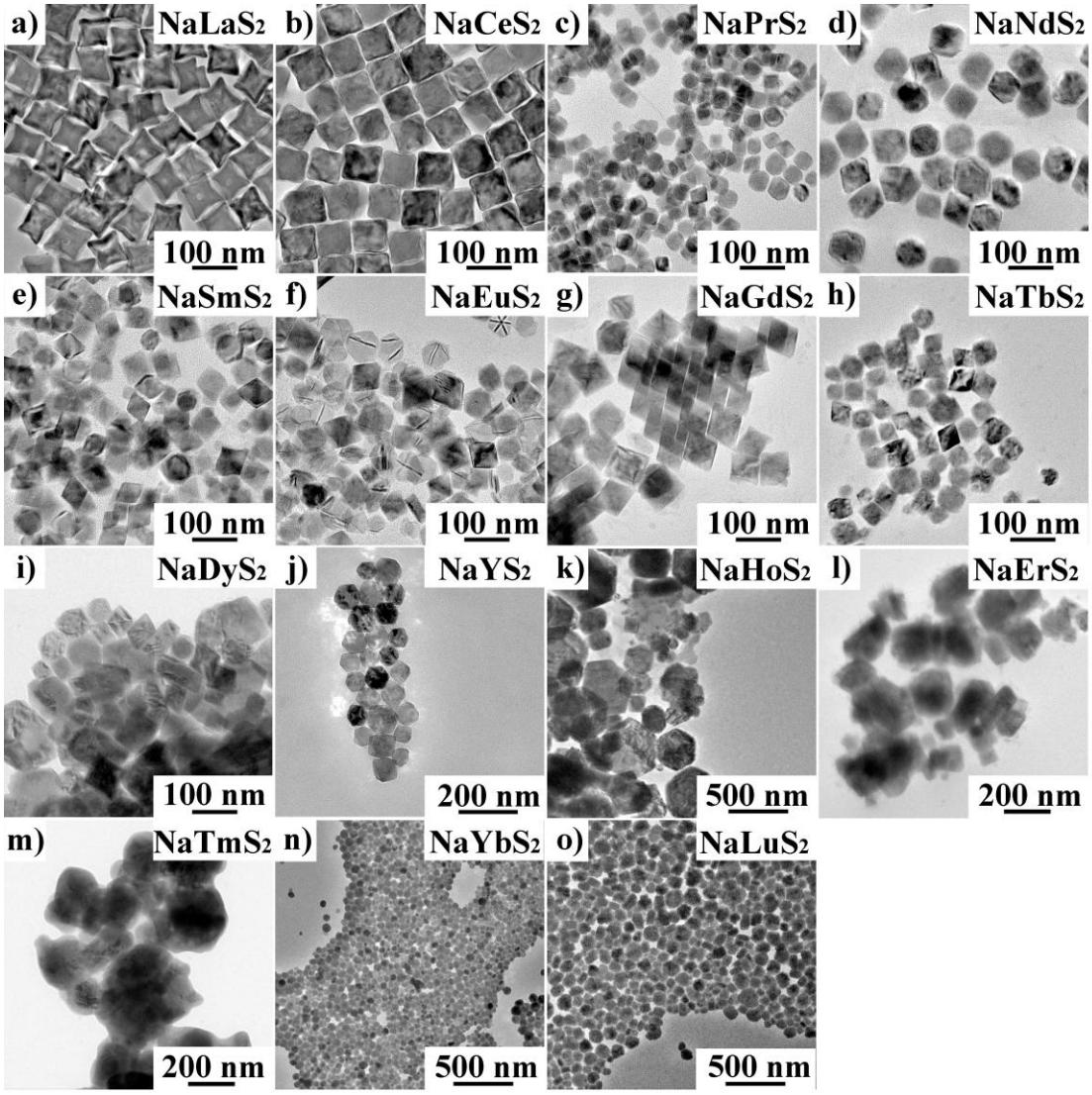

Figure S5. TEM images of $NaRES_2$ (RE = La~Lu, Y) NCs.

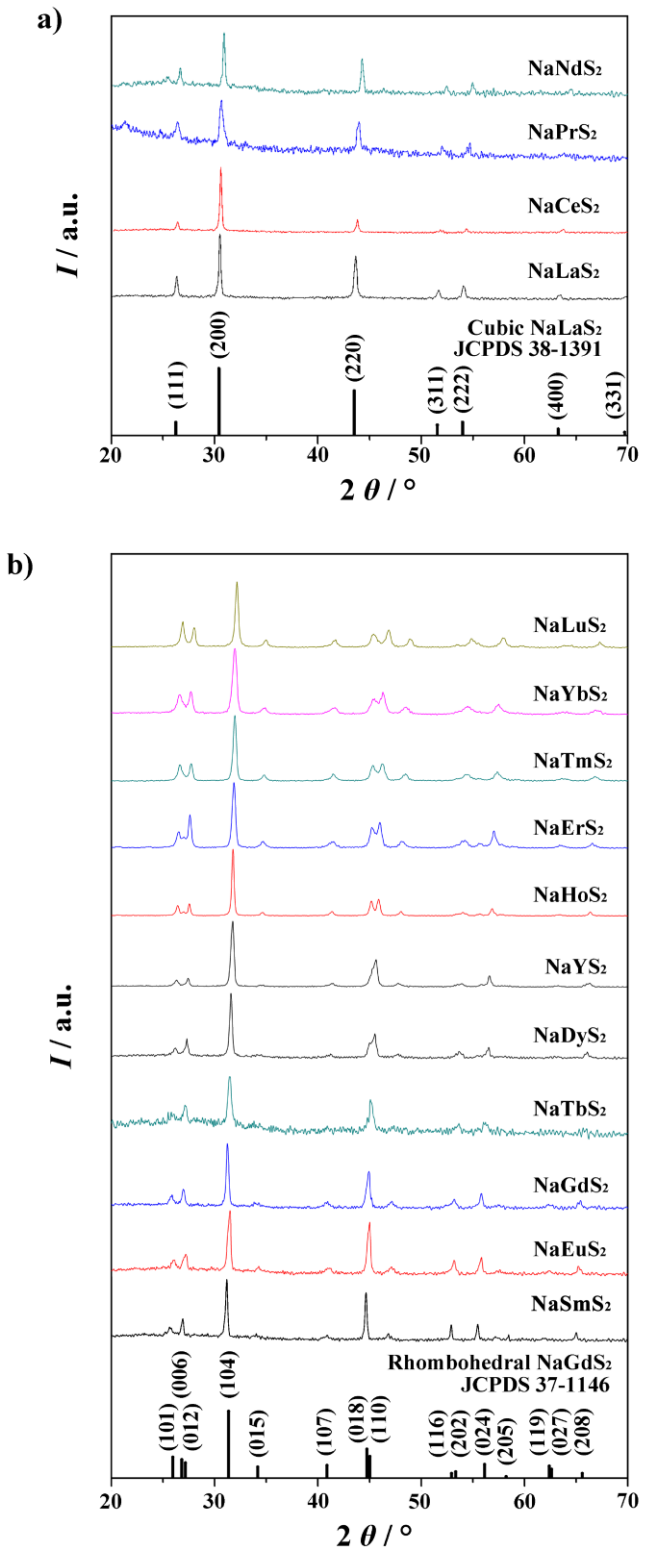

Figure S6. X-ray Diffraction (XRD) patterns of $NaRES_2$ (RE = La~Lu, Y) NCs in a) cubic phase and b) rhombohedral phase (compared with the standard XRD patterns of cubic $NaLaS_2$ (JCPDS 38-1391) and rhombohedral $NaGdS_2$ (JCPDS 37-1146), respectively).

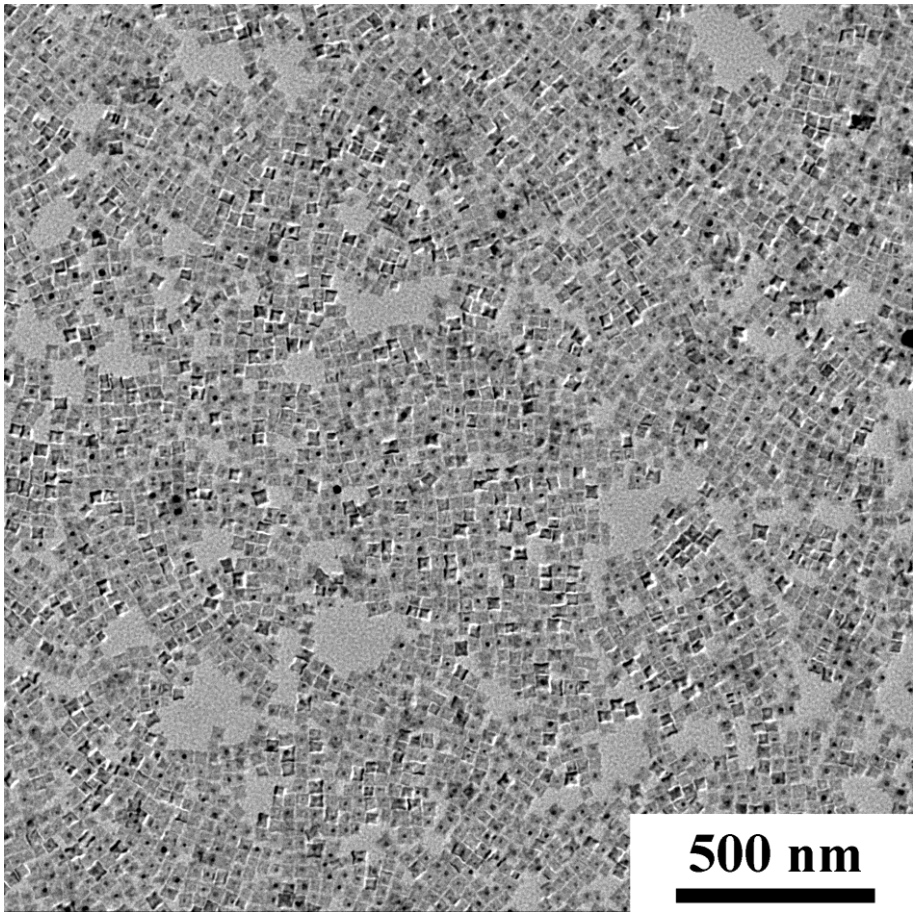

Figure S7. Large area TEM image of Au@$NaLaS_2$ NCs.

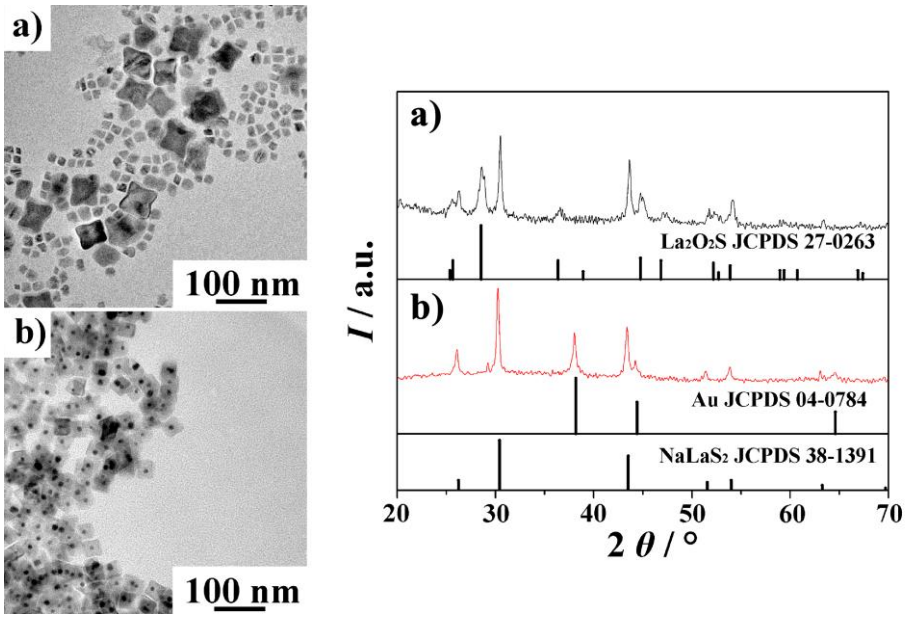

Figure S8. TEM images (left) and corresponding XRD spectra (right) of a) mixture of $NaLaS_2$ NCs and Na-doped La_2O_2S nanoplates and b) Au@$NaLaS_2$ NCs. The samples above were prepared following Method I except that only 3 mmol of Na(acac) was used.

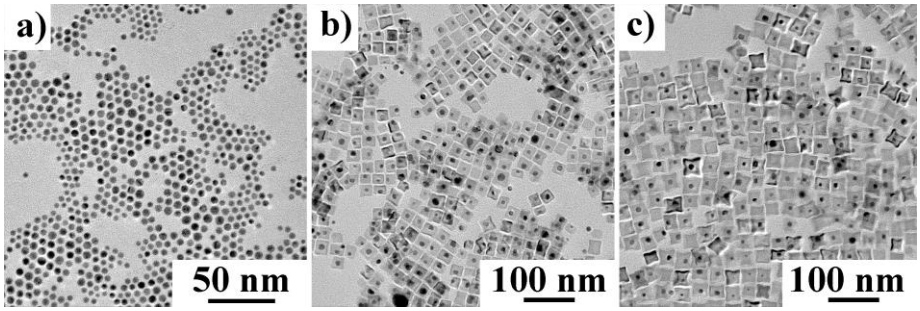

Figure S9. TEM images of a) initial Au cores and b)-c) Au@$NaLaS_2$ nanostructure. The amount of Au cores used for synthesis Au@$NaLaS_2$ NCs was b) 10 mg and c) 5 mg, respectively. The sizes of the Au cores and Au@$NaLaS_2$ NCs in every sample were listed in Table S1.

Table S1. The diameters of Au cores, edge-length of Au@$NaLaS_2$ NCs and the average thickness of $NaLaS_2$ shells in samples shown in Figure S9 (Unit: nm).

Samples	Diameter of Au cores	Edge-length of Au@$NaLaS_2$ NCs	Average thickness of $NaLaS_2$ shells
Au cores	5.2 ± 0.6	--	--
Au@$NaLaS_2$ NCs (10 mg Au cores)	8.5 ± 0.8	20.4 ± 2.0	6.0 ± 1.5
Au@$NaLaS_2$ NCs (5 mg Au cores)	9.3 ± 1.1	29.2 ± 2.2	10.0 ± 1.2

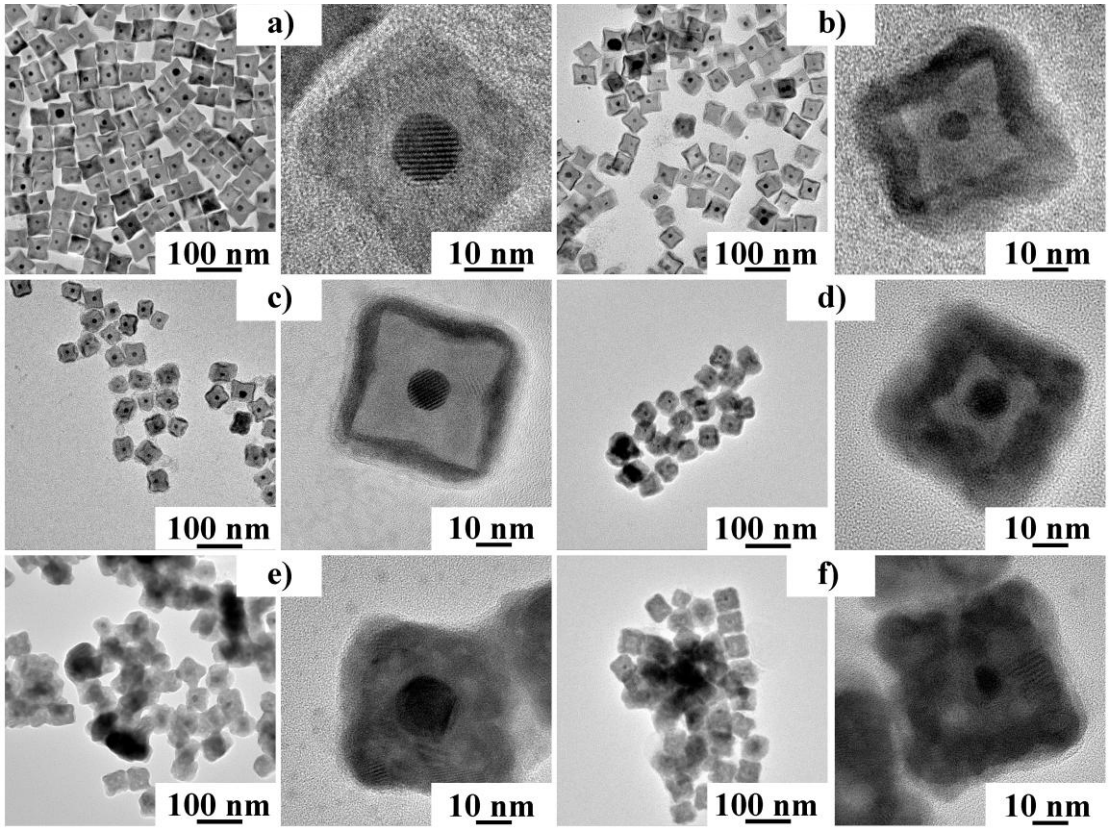

Figure S10. TEM images of a) initial Au@$NaLaS_2$ nanocubes and b)-f) Au@$NaLaS_2$@Ag_2S nanocubes with different thickness of Ag_2S shells. The volume ratios between $AgNO_3$ stock solution and Au@$NaLaS_2$ NCs dispersion was b) 1:1, c) 3:1, d) 5:1, e) 10:1 and f) 14:1.

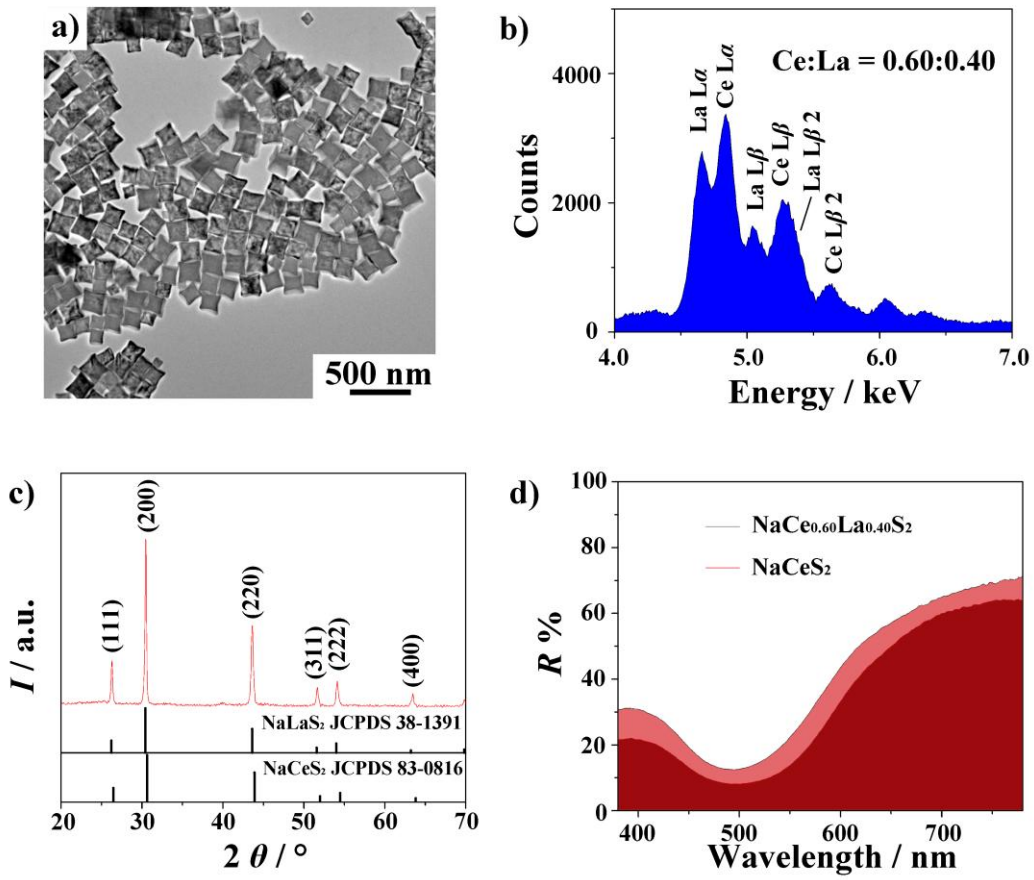

Figure S11. a) TEM image and b) EDX analysis of $NaCe_xLa_{1-x}S_2$ nanocubes. EDX analysis show the mole ratio between Ce and La in $NaCe_xLa_{1-x}S_2$ nanocubes was 0.60:0.40. c) XRD spectrum of $NaCe_xLa_{1-x}S_2$ nanocubes compared with standard XRD patterns of cubic $NaCeS_2$ (JCPDS 83-0816) and cubic $NaLaS_2$ (JCPDS 38-1391). d) Diffuse reflection spectrum of $NaCe_xLa_{1-x}S_2$ nanocubes (light red) compared with the one of $NaCeS_2$ nanocubes (dark red). The dopant of La in $NaCeS_2$ NCs decreases the absorption around all the wavelengths and increases the lightness of the color of the nanosized pigment. The color coordinates were calculated from the diffuse reflection spectrum and listed in Table S2.

Table S2. The comparison of the color coordinates between $NaCeS_2$ NCs and $NaCe_{0.60}La_{0.40}S_2$ NCs.

Color coordinates	*L**	*a**	*b**	*C**
$NaCeS_2$	54.0	41.1	18.7	45.1
$NaCe_{0.60}La_{0.40}S_2$	62.2	37.1	19.8	42.1

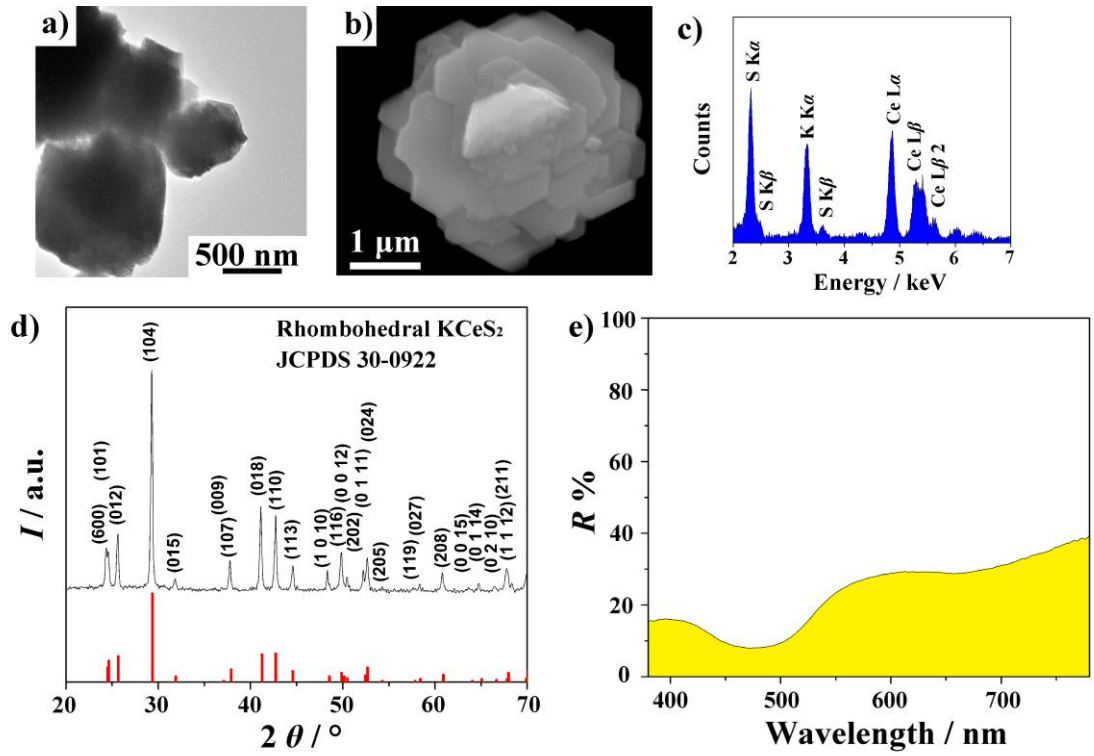

Figure S12. a) TEM and b) SEM images, and c) EDX analysis of $KCeS_2$ micro-crystals. d) XRD spectrum of $KCeS_2$ micro-crystals compared with the standard XRD pattern of rhombohedral $KCeS_2$ (JCPDS 30-0922). d) Diffuse reflection spectrum of $KCeS_2$ micro-crystals. The color coordinates were calculated from the diffuse reflection spectrum and listed in Table S3.

Table S3. Color coordinates of the as-obtained $KCeS_2$ micro-crystals.

Color coordinates	*L**	*a**	*b**	*C**
$KCeS_2$	56.2	15.1	30.7	34.2

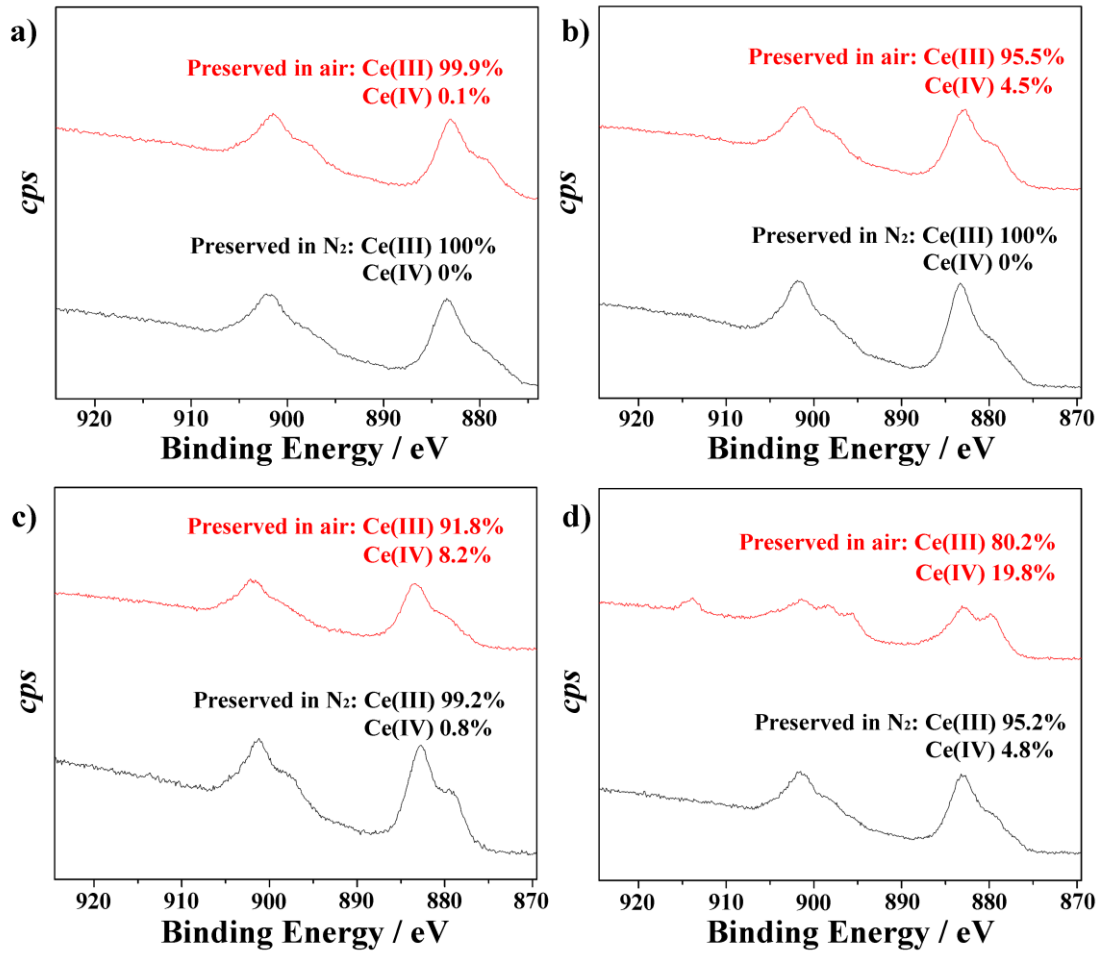

Figure S13. X-ray photoelectron spectroscopy (XPS) analyses of Ce 3d electrons in $NaCeS_2$ nanocubes with edge-length of a) 204 nm, b) 76 nm, c) 41 nm and d) 12.2 nm. Black lines represent XPS spectra of samples preserved in N_2 and red lines represent XPS spectra of samples preserved in air for 7 days. XPS analyses show the ratios between Ce(III) and Ce(IV) in all the samples. Only the XPS spectrum of the smallest $NaCeS_2$ NCs preserved in air for 7 days shows an obvious signal of Ce(IV) around B.E. = 915 eV.

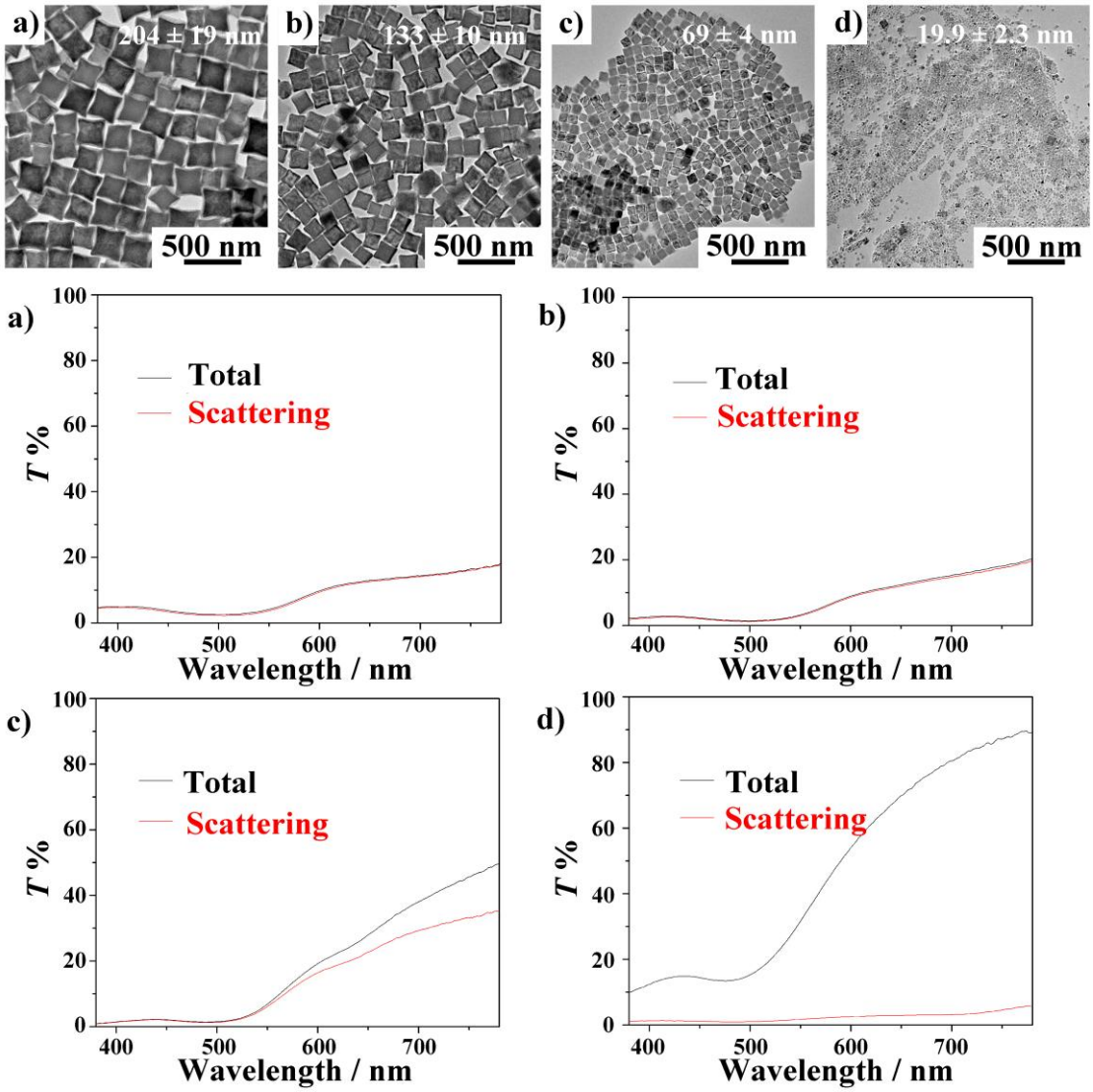

Figure S14. TEM images (top) and corresponding total transmission (black lines) and scattering transmission (red lines) spectra (bottom) of cyclohexane dispersions of $NaCeS_2$ nanocubes with average edge length of a) 204 nm, b) 133 nm, c) 69 nm and d) 19.9 nm. Direct transmission spectra can be obtained by deducting the scattering transmission spectra from total transmission spectra. The concentration of $NaCeS_2$ NCs in each dispersion was 0.5 mg/mL.

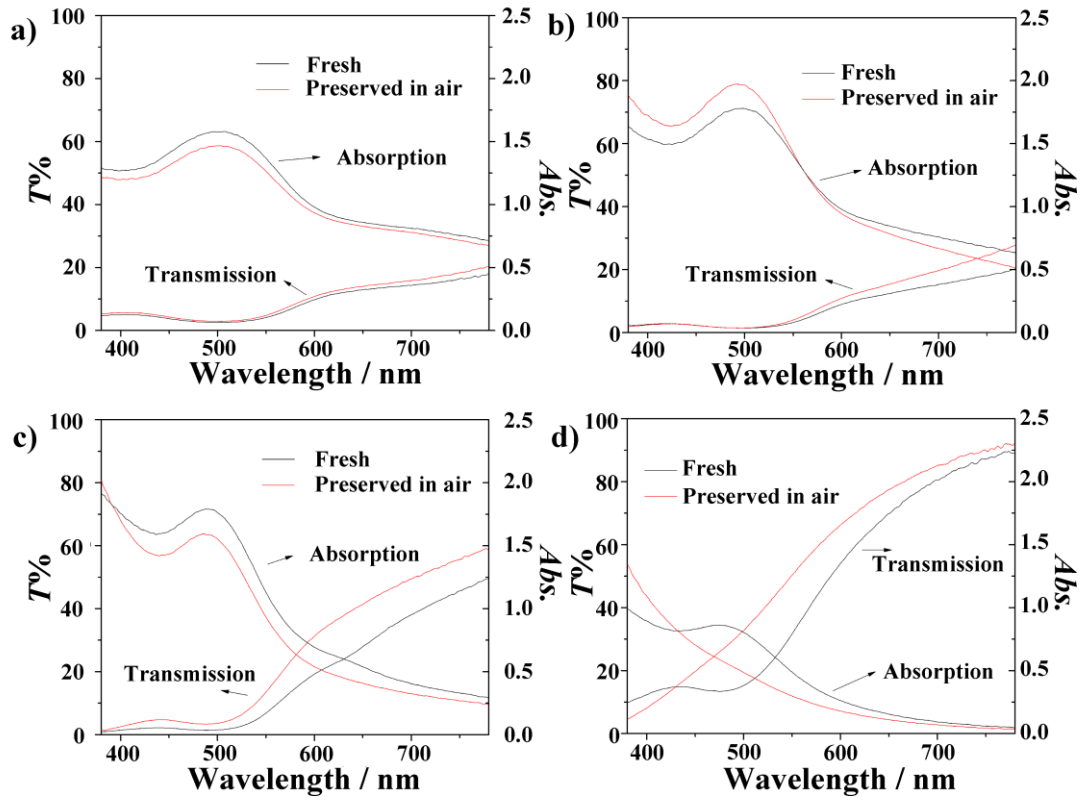

Figure S15. Transmission and absorption spectra of cyclohexane dispersions of $NaCeS_2$ nanocubes with edge-length of a) 204 nm, b) 133 nm, c) 69 nm and d) 19.9 nm. Blue lines show the spectra for fresh dispersions and red lines show the spectra for dispersions preserved in colorimetric tubes for a) – c) a month and d) one day. The red lines of cyclohexane dispersions of $NaCeS_2$ NCs with edge-length larger than 70 nm do not show obvious changes compared with blue lines. These dispersions were stable in air. The increase of the transparency of red lines can be ascribed to the decrease of the concentration of $NaCeS_2$ nanocubes caused by the absorption of nanoparticles on the glass wall. As to the cyclohexane dispersion of $NaCeS_2$ nanocubes with side-length of 19.9 nm preserved for 1 day, the main absorption peak around λ = 500 nm disappeared and the color turned from red to dark yellow. The concentration of $NaCeS_2$ NCs in each dispersion was 0.5 mg/mL.